JOURNAL OF THERMOPHYSICS AND HEAT TRANSFER
Vol. 11, No. 2, April–June 1997

Rarefaction Effects in Small Particle Combustion

Robert Hiers*
Sverdrup Technology, Inc., Arnold Air Force Base, Tennessee 37389-9013

The standard theories of particle combustion rely upon continuum gasdynamic relationships. These theories predict that small reacting particles are always essentially in thermal equilibrium with the ambient gas phase. This is a consequence of three results from continuum theory: 1) the convective loss is inversely proportional to particle size, 2) the convective loss is independent of pressure, and 3) the convective loss depends upon the thermal conductivity of the ambient gas. Typical soot particles are smaller than the mean free path of the ambient gas. Energy and mass conservation equations are derived assuming free molecular conditions. Under these assumptions, the convective loss is shown to be independent of particle size, dependent on the ambient pressure, and independent of the gas phase thermal conductivity. These equations are solved for a variety of $O_2/O/N_2$ gas mixtures, pressures, and temperatures. High O_2 mole fractions at low pressure result in significant gas/particle thermal nonequilibrium. The particle surface temperature is shown to elevate significantly above the gas temperature. This result contradicts the behavior of small reacting particles predicted by continuum theory.

Nomenclature

A = particle surface area
C = particle specific heat
D = particle diameter
E = particle internal energy
e = particle specific internal energy
f = collision efficiency
h = convective heat transfer coefficient
h_{fm} = free molecular convective heat transfer coefficient
$h_f^0(0)$ = enthalpy of formation at 0 K
k = Boltzmann constant
k_f = gas film thermal conductivity
k_r = temperature-dependent constant in particle emissivity
m = gas molecular mass
$\tilde{m}$ = mass of carbon atoms removed from particle per reactive collision
n = number density
P_{O_2} = oxygen partial pressure
P_∞ = ambient pressure
$\dot{Q}$ = heat transfer rate from the gas to the particle
q_{nr} = energy transferred to the particle by a nonreactive collision
q_r = energy transferred to the particle by a reactive collision
$\mathcal{R}$ = specific gas constant
r = particle radius
T = particle temperature
T_0 = reference temperature
T_∞ = ambient temperature
t = time
u = internal energy
V = particle volume
$\bar{v}$ = average molecular velocity
X = stoichiometric coefficients
Z = total collision frequency
α = surface thermal accommodation coefficient
γ = ratio of specific heats
ε = emissivity
λ = mean free path
μ = gas kinematic viscosity
ρ = particle material density
ρ_∞ = ambient density
σ = Stefan–Boltzmann constant
ω = specific oxidation rate

Presented as Paper 96-1892 at the AIAA 31st Thermophysics Conference, New Orleans, LA, June 17–20, 1996; received July 23, 1996; revision received Nov. 1, 1996; accepted for publication Nov. 1, 1996. This paper is declared a work of the U.S. Government and is not subject to copyright protection in the United States.

*Senior Engineer, Arnold Engineering Development Center Group. Senior Member AIAA.

Introduction

MOST developments of the governing equations of soot oxidation focus on the diffusion (large particle, high temperature) or kinetic (small particle, low temperature) limits.[1–5] In a seminal paper, Libby and Blake[6] developed the general kinetic and diffusive equations governing the oxidation of carbon spheres. In the limit of small particles, all of these developments predict that the particles are essentially in thermal equilibrium with the gas. Figure 1 illustrates the temperature profiles resulting from diffusionally and kinetically limited combustion. For large particles (diffusion limit), the particle temperature can rise significantly above the ambient gas temperature. For small particles (kinetic limit), the thermal conduction loss to the surrounding gas is predicted to overwhelm the energy release at the particle surface. Indeed, in most shock-tube studies[7–10] of soot oxidation, the experimenters assumed that the particle temperature could be computed from the shock-tube relations. Roth et al.[9] explicitly states: "The particle surface temperature was assumed to be equal to the gas phase temperature. This assumption seems to be reasonable for nm-size shock-heated, reacting particles." It is precisely this assumption that is investigated in this paper.

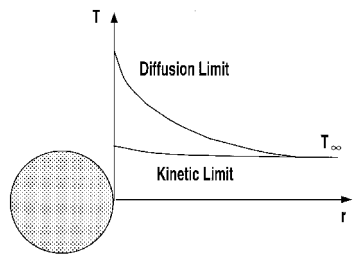

Fig. 1 Kinetically and diffusionally controlled combustion.

Continuum and Free Molecular Convection Heat Transfer Coefficients

Consider a nonreacting sphere undergoing convective heat transfer with a surrounding gas. The governing heat transfer equation is

$$\dot{Q} = hA(T_\infty - T) \tag{1}$$

If continuum conditions are assumed (as is done in Refs. 1–6), then Nu will be approximately 2, since the particle is undergoing free convection.[11,12] Since Nu is defined as

$$Nu = hD/k_f \tag{2}$$

then we have the classic result

$$h = k_f/r \tag{3}$$

For small particles the convective coefficient is extremely large and forces the particle temperature to rapidly approach the gas temperature. This is the result cited frequently in the literature to justify thermal equilibrium for small particles, even in the presence of energy addition by oxidation. Recall that the thermal conductivity of a gas is not dependent on pressure.[13] Therefore, the continuum convective coefficient is independent of pressure.

If the characteristic body dimension is small compared to the mean free path, the body is in free molecular flow, and the convective heat transfer is given by[14,15]

$$-\dot{Q} = \alpha \rho_\infty \mathcal{R} T_\infty \sqrt{\frac{\mathcal{R}T_\infty}{2\pi}} \left[\frac{\gamma}{\gamma - 1} - \frac{\gamma + 1}{2(\gamma - 1)} \frac{T}{T_\infty} - \frac{1}{2} \right] A \tag{4}$$

This assumes a Maxwellian velocity distribution in the gas as a whole and no mean relative velocity between the gas and the particle. It also assumes that the internal energy modes are fully excited and in equilibrium with the translational energy. By rearranging and invoking the ideal gas law we arrive at

$$\dot{Q} = \frac{\alpha}{2} \frac{P_\infty}{T_\infty} \sqrt{\frac{\mathcal{R}T_\infty}{2\pi}} \frac{\gamma + 1}{\gamma - 1} A(T_\infty - T) \tag{5}$$

This is in agreement with an early work of Simmons and Spadaro.[16]

By comparison with Eq. (1) we can define h_{fm} as

$$h_{\text{fm}} = \frac{\alpha}{2} \frac{P_\infty}{T_\infty} \sqrt{\frac{\mathcal{R}T_\infty}{2\pi}} \frac{\gamma + 1}{\gamma - 1} \tag{6}$$

Comparing Eq. (6) with Eq. (3), we see that the $1/r$ dependence does not appear in the free molecular heat transfer coefficient. Therefore, small particle size does not result in large convective coefficients. Indeed, the free molecular heat transfer coefficient is independent of particle size, but is instead dependent on pressure (or on more physical grounds, density). Also note that the gas thermal conductivity does not appear. The exact opposite dependencies are seen for the continuum heat transfer coefficient. Therefore, significantly different behavior might be expected under free molecular conditions.

We can now make a direct comparison of the free molecular and continuum convective heat transfer coefficients by forming the ratio h/h_{fm} and plotting this ratio as a function of temperature and pressure (see Fig. 2). A 50-nm-diam particle immersed in molecular oxygen is used for this calculation. The NASA Equilibrium Code with Transport Properties[17] is used to provide the temperature-dependent ratio of specific heats. The accommodation coefficient is assumed to be unity. For these conditions, the free molecular convective heat transfer coefficient is always significantly less than the continuum convective coefficient. At 0.1 atm, the continuum coefficient is 500–1000 times larger than the free molecular coefficient. If the particle is actually in free molecular conditions, the use of the continuum heat transfer coefficient will significantly overpredict the heat transfer rate from the particle, implying an underprediction of the particle temperature.

Soot Particle *Kn*

The particle Kn is defined as the ratio of the mean free path of the gas to the particle diameter, or[18]

$$Kn = \lambda/D \tag{7}$$

where λ is defined by

$$\lambda = \frac{2\mu}{P_\infty} \left(\frac{\pi k T_\infty}{8m} \right)^{1/2} \tag{8}$$

The definition of flow regimes is problem-dependent, but in general for low mean velocities[15]: $Kn < 0.1$, continuum flow; $0.1 < Kn < 2.0$, slip flow; $2.0 < Kn < 10$, transitional flow; and $Kn > 10$, free molecular flow.

Assuming again that the particle is immersed in pure molecular oxygen, the NASA Equilibrium Code with Transport Properties[17] is used to provide the viscosity so that Kn as a function of temperature and pressure can be computed assuming a baseline particle diameter of 50 nm. This will be a baseline Kn only, since the particle size is held constant. The particle size will, of course, decrease with oxidation, causing an increase in the Kn. Figure 3 is a plot of particle Kn as a function of oxygen pressure and temperature. Note that the particle Kn is always much greater than 1.0, even at atmospheric pressure. At 0.1 atm, the Kn is greater than 100. Therefore, the particles are always in transitional to free molecular flow. Rarefaction effects will always be important, and continuum relations may fail.

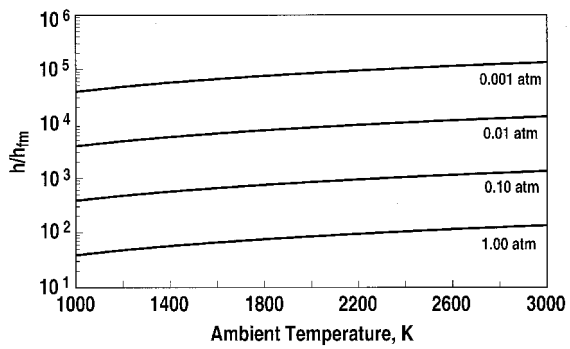

Fig. 2 Ratio of convective heat transfer coefficients.

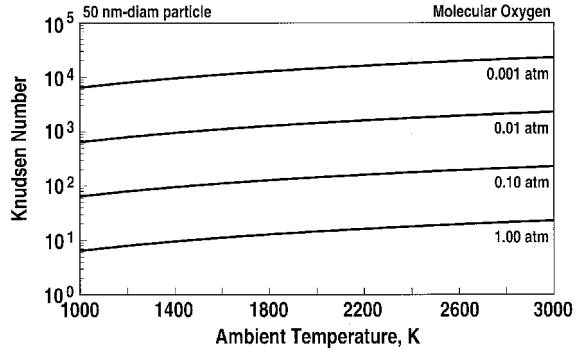

Fig. 3 Particle *Kn*.

Particle Energy Equation

If we denote the particle thermal energy as E, then E is given by

$$E = \rho V(t) e(t) \tag{9}$$

Because particle volume is simply $4/3\,\pi r^3$, then E is a function of both r and T. Since both r and T are functions of time, then the rate of change of E is

$$\frac{\mathrm{d}E}{\mathrm{d}t} = \frac{\partial E}{\partial T}\frac{\mathrm{d}T}{\mathrm{d}t} + \frac{\partial E}{\partial r}\frac{\mathrm{d}r}{\mathrm{d}t} \tag{10}$$

We can write the internal energy as

$$e = \int_{T_0}^{T} C\,\mathrm{d}\hat{T} + e(T_0) \tag{11}$$

Additionally, it can be shown that

$$\frac{\partial E}{\partial T} = \rho V C \tag{12}$$

If we use the thermodynamic properties of graphite (a reference element) for soot, then $e(T_0)$ is defined to be zero. Throughout this paper, the reference temperature is assumed to be 0 K. We can also find

$$\frac{\partial E}{\partial r} = \frac{\partial}{\partial r}\left(\rho V \int_0^T C\,\mathrm{d}\hat{T}\right) = \rho A e \tag{13}$$

If we assume we are given the specific oxidation rate, ω (g/cm^2/s), as a function of temperature and pressure, we can find the rate of change of the particle radius since

$$-\omega A = \rho\frac{\mathrm{d}V}{\mathrm{d}t} = \rho A\frac{\mathrm{d}r}{\mathrm{d}t} \tag{14}$$

or

$$\frac{\mathrm{d}r}{\mathrm{d}t} = -\frac{\omega}{\rho} \tag{15}$$

Substituting Eqs. (12), (13), and (15) into Eq. (10), and rearranging, yields

$$\frac{\mathrm{d}E}{\mathrm{d}t} = A\left(\frac{\rho r}{3} C\frac{\mathrm{d}T}{\mathrm{d}t} - \omega e\right) \tag{16}$$

This is the rate of change of the energy content of the particle.

Reactive and Nonreactive Collisions

The free molecular model is one of collision counting. A collision that results in an exothermic reaction adds energy to the particle. An endothermic reaction removes energy. Nonreactive collisions will either add or subtract energy from the particle: adding if the gas is hotter than the particle, subtracting if the particle is hotter than the gas. Also, if a reaction occurs, mass must be removed from the particle.

If the characteristic body dimension is small compared to the mean free path, the body is in free molecular flow, and heat transfer will occur only by direct collisions with the ambient gas molecules[15] (ignoring radiation for the moment). Upon collision with the particle surface, the gas molecules will exchange energy with the surface, either by transferring internal energy, or by chemically reacting with the surface. We can express the oxidation rate ω as a fraction of the total number of collisions; i.e.,

$$\omega = Zf\tilde{m} \tag{17}$$

Assuming no relative motion between the particle and the gas (dynamic equilibrium), Z is given by[13]

$$Z = \tfrac{1}{4} n\bar{v} = \tfrac{1}{4}(P_\infty/kT_\infty)\sqrt{8kT_\infty/\pi m} \tag{18}$$

The energy flux at the particle surface caused by collisions with gas molecules is given by

$$\frac{\mathrm{d}E}{\mathrm{d}t} = [Zfq_r + Z(1-f)q_{\mathrm{nr}}]A \tag{19}$$

The energy u has contributions from translational energy, internal structure (e.g., vibrational and rotational energy), and chemical potential energy (bond energy). We can write the internal energy of the gas molecules as

$$u = u_{\mathrm{translational}} + u_{\mathrm{internal}} + u_{\mathrm{chemical}} \tag{20}$$

Since the particle is smaller than the mean free path, the molecular flux to the particle surface is effusive. Therefore, the average translational energy of gas molecules incident on the particle surface is $2kT$.[14] Also, since the reference temperature is chosen as 0 K, the chemical potential energy is simply the enthalpy of formation at 0 K, or $h_f^o(0)$. Therefore, the internal energy at any T is[19]

$$u(T) = 2kT + \int_0^T C_{v,\mathrm{internal}}\,\mathrm{d}\hat{T} + h_f^o(0) \tag{21}$$

where $C_{v,\mathrm{internal}}$ is the contribution of rotation, vibration, and electronic structure to the specific heat at constant volume.

The change in the internal energy during a collision is given by

$$\Delta u = u_{\mathrm{products}} - u_{\mathrm{reactants}}$$

or, using Eq. (21)

$$\Delta u = \sum_{i\,\mathrm{products}} X_i\left\{2kT_i + \int_0^{T_i}(C_{v,\mathrm{internal}})_i\,\mathrm{d}\hat{T} + [h_f^o(0)]_i\right\} - \sum_{j\,\mathrm{reactants}} X_j\left\{2kT_j + \int_0^{T_j}(C_{v,\mathrm{internal}})_j\,\mathrm{d}\hat{T} + [h_f^o(0)]_j\right\} \tag{22}$$

Equation (21) can be used to find the change in internal energy for either reactive or nonreactive collisions. By the First Law of Thermodynamics, the energy transferred to the particle during the collision is simply the negative of the change in internal energy of the collision. Therefore, for a nonreactive collision

$$q_{\mathrm{nr}} = -\Delta u_{\mathrm{nr}} \tag{23}$$

and for a reactive collision

$$q_r = -\Delta u_r \tag{24}$$

The JANNAF Thermochemical Tables[20] and associated curve fits[17] were used for all specific heats and heats of formation.

Free Molecular Energy Equation

Equation (19) represents the flux of energy at the particle surface caused by collisions with ambient gas molecules. The

particle will also exchange energy with the environment by radiation. The rate of radiant energy transfer is given by

$$\left(\frac{dE}{dt}\right)_{\text{radiation}} = \varepsilon\sigma(T_\infty^4 - T^4)A \tag{25}$$

Since small particles are mass (or volume) radiators,[21] the ε is proportional to the particle radius. Therefore

$$\left(\frac{dE}{dt}\right)_{\text{radiation}} = rk_r\sigma(T_\infty^4 - T^4)A \tag{26}$$

where k_r is a function of particle temperature and is derived from the Lee and Tien[21] soot optical properties. The total energy flux at the particle surface is therefore the sum of Eqs. (26) and (19), or

$$\frac{dE}{dt} = [Zfq_r + Z(1-f)q_{\text{nr}}]A + rk_r\sigma(T_\infty^4 - T^4)A \tag{27}$$

Substituting Eq. (17) into Eq. (16) yields

$$\frac{dE}{dt} = A\left(\frac{\rho r}{3}C\frac{dT}{dt} - Zf\tilde{m}e\right) \tag{28}$$

Equating Eqs. (27) and (28) and solving for the rate of change of temperature yields

$$\frac{dT}{dt} = \frac{3Z}{\rho rC}[f(\tilde{m}e + q_r) + (1-f)q_{\text{nr}}] + \frac{3k_r\sigma}{\rho C}(T_\infty^4 - T^4) \tag{29}$$

In free molecular flow the heat transfer is independent of the gas phase thermal conductivity, whereas the continuum heat transfer rate is linearly dependent on the thermal conductivity. In free molecular flow, there is no extra $(1/r)$ term on the convective loss rate. Therefore, the convective loss term will not automatically dominate the heat addition term for small particles. Heat transfer processes (except radiation) are limited by the collision rate Z. This means that the convective heat transfer is linearly dependent on pressure, whereas in continuum flow the convective heat transfer is independent of pressure.

Note that the radius r appears in Eq. (29) as an unknown function of time. However, substituting Eq. (17) into Eq. (15) yields an ordinary differential equation (ODE) for the particle radius

$$\frac{dr}{dt} = \frac{-Zf\tilde{m}}{\rho} \tag{30}$$

Since f is also a function of particle temperature, Eqs. (29) and (30) form a coupled set of ODEs for the particle temperature and radius as functions of time. These equations are statements of energy conservation and mass conservation, respectively. These equations were integrated in time using a modified implicit Euler method. The time step is varied to assess both stability and accuracy of the calculations.

Soot Oxidation Rates

Oxidation by Molecular Oxygen

A summary of soot oxidation rate measurements over a wide range of oxygen partial pressure appears in Fig. 4. The data have been cast into the form of collision efficiency, assuming the reaction

$$2C(s) + O_2 \Rightarrow 2CO$$

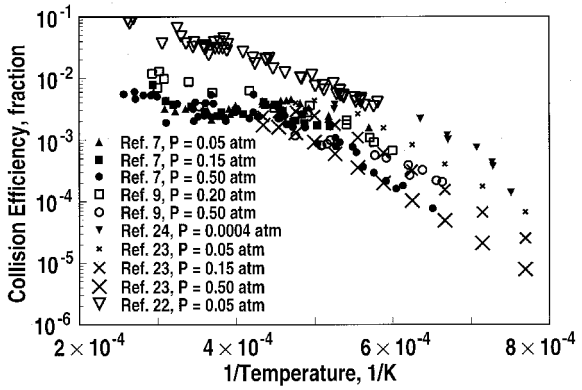

Fig. 4 Collision efficiency for $2C(s) + O_2 = 2CO$.

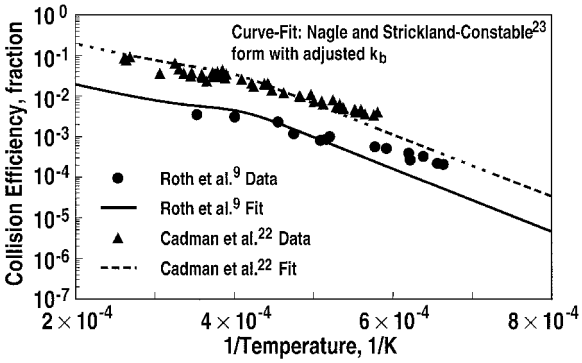

Fig. 5 Curve fit of collision efficiency for $2C(s) + O_2 = 2CO$.

Shock-tube data from Park and Appleton,[7] Roth et al.,[9] and Cadman et al.,[22] are compared with the carbon rod data from Nagle and Strickland-Constable,[23] and the low-pressure flow tube data of Rosner and Allendorf.[24] Park and Appleton,[7] Roth et al.,[9] and Cadman et al.[22] used thermal or lamp black particles, and Rosner and Allendorf[24] used graphite filaments. Roth et al.[9] and Olander et al.[25,26] independently confirmed that the reaction forming CO is much more likely than that forming CO_2. Roth et al.[9] used laser absorption to confirm the presence of CO and the absence of CO_2. Olander et al.[25,26] used mass spectrometry to determine that the reaction forming CO was at least two orders of magnitude more probable than that forming CO_2. The Cadman et al.[22] data lie well above most of the other data, but fair in nicely with the Rosner and Allendorf[24] measurements. The data in Fig. 4 illustrate the wide range of experimental oxidation rates reported in the literature. Different experimental techniques and different carbon samples (soot, graphite powder, etc.) contribute to the spread in the data. Figure 5 presents the Cadman et al.[22] and Roth et al.[9] data (at oxygen partial pressures of 0.05 and 0.5 atm, respectively) along with a fit to these data using an equation of the Nagle and Strickland-Constable[23] form:

$$f = \frac{\omega}{Z\tilde{m}} = \frac{12}{Z\tilde{m}}\left[\left(\frac{k_A P_{O_2}}{1 + k_Z P_{O_2}}\right)\chi + k_B P_{O_2}(1-\chi)\right] \quad \text{dimensionless}$$

where

$$\chi = \left(1 + \frac{k_T}{k_B P_{O_2}}\right)^{-1}$$

$$k_A = 20\ \exp(-15{,}100/T),\ \text{g cm}^{-2}\ \text{s}^{-1}\ \text{atm}^{-1}$$

$$k_B = 0.2\ \exp(-7640/T),\ \text{g cm}^{-2}\ \text{s}^{-1}\ \text{atm}^{-1} \tag{31}$$

$$k_T = 1.51 \times 10^5\ \exp(-48{,}800/T),\ \text{g cm}^{-2}\ \text{s}^{-1}$$

$$k_Z = 21.3\ \exp(2060/T),\ \text{atm}^{-1}$$

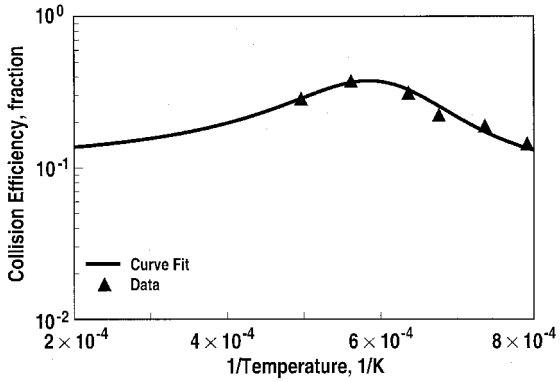

Fig. 6 Rosner and Allendorf[24] collision efficiency for C + O = CO.

The Roth et al.[9] data are well fit with a coefficient on k_B of 0.02. In the original Nagle and Strickland-Constable[23] work, the coefficient on k_B is 0.00446. This is the only change to the original Nagle and Strickland-Constable[23] fit.

Oxidation by Atomic Oxygen

Rosner and Allendorf[24] measured the rate of O-atom attack on pyrolytic graphite surfaces in a flow tube at low pressure. This data, along with a polynomial curve fit, are shown in Fig. 6. These collisions are extremely efficient, with a reaction probability near 1.0. Rosner and Allendorf[27] also confirmed the product of the reaction with atomic oxygen as CO. Since the atomic oxygen collisions are so efficient, and since the expected atomic oxygen content is small, this collision efficiency is assumed to be independent of atomic oxygen partial pressure.

Model Results

Now that we have collision efficiencies for more than one reaction, the energy and mass conservation equations [Eqs. (28) and (29)] must be extended to consider more than one collision partner. Assuming simple superposition of the collisions yields

$$\frac{dT}{dt} = \frac{3}{\rho r C}\sum_i Z_i[f_i(\tilde{m}_i e + q_{r_i}) + (1 - f_i)q_{\mathrm{nr}_i}] + \frac{3k_r\sigma}{\rho C}(T_\infty^4 - T^4) \tag{32}$$

$$\frac{dr}{dt} = \frac{-1}{\rho}\sum_i (Zf\tilde{m})_i \tag{33}$$

where the summation is taken over the number of collision partners. Three collision partners will be considered: O_2, O, and N_2. Of course, every collision with N_2 will be nonreactive, i.e., f is identically zero for N_2. Equations (32) and (33) represent the current model for a soot particle reacting in an arbitrary gas mixture.

Because of the competition among the reactive collision partners for active sites on the surface of the soot particle, superposition is not precisely valid. However, it does provide an upper bound on the reaction rate for a mixture of reactive collision partners.

Oxidation in O_2, O_2/N_2, and O_2/O Mixtures

Figure 7 presents a temperature history for a 50-nm soot particle oxidizing in pure O_2 at a pressure of 0.02 atm. The particle is assumed initially to be in equilibrium with the 2000-K bath gas. In all calculations, the stated bath gas composition is frozen, i.e., no equilibrium dissociation of O_2 into O_2, and O is considered. The oxidation rates of Cadman et al.,[22] Roth et al.,[19] and Nagle and Strickland-Constable[23] are used. The Cadman et al.[22] rates produce the maximum thermal nonequilibrium. Note that the maximum temperature elevation of the particle temperature above the gas temperature is over 400 K when the Cadman et al.[22] rates are used. The reduction in particle diameter as a function of time is shown in Fig. 8. Note that the temperature elevation is over 300 K when the particle has lost less than 50% of its mass for the Cadman et al.[22] rates. Even for the Nagle and Strickland-Constable[23] rates the particle temperature elevation is about 50 K. It is important to note that, if the typical continuum mass and energy conservation equations are used, the computed temperature elevation is a few degrees at most for particles of this size. Therefore, small particle size does not guarantee gas/particle thermal equilibrium for reacting particles. In fact, it is the small particle size that allows thermal nonequilibrium, if rarefaction effects are properly taken into account. This result contradicts the small particle limit predicted by the continuum theory in Refs. 1–6.

Figure 9 presents the particle temperature elevation at burnout for a 50-nm-diam particle oxidizing in various O_2/N_2 mixtures at 1.00 atm. Here, particle burnout is defined as the time at which the particle diameter reduces to 0.5 nm. These and all later calculations use the Cadman et al.[22] rates for O_2

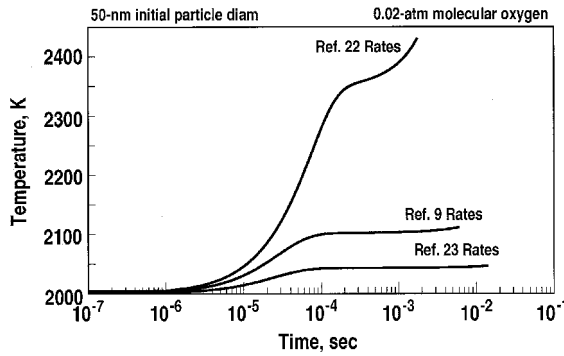

Fig. 7 Particle temperature history.

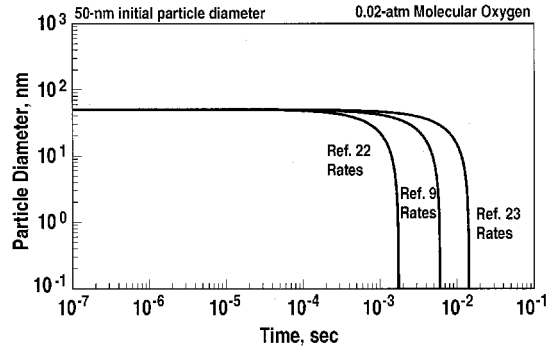

Fig. 8 Particle size history.

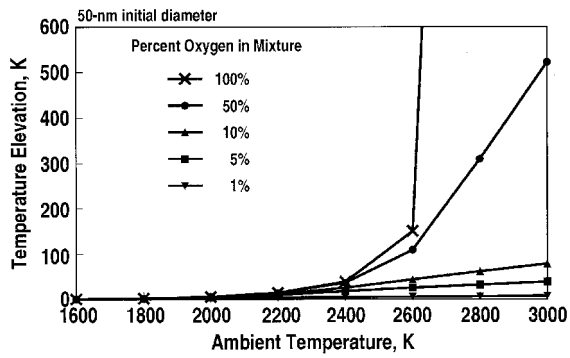

Fig. 9 Particle temperature elevation at burnout for 1.00-atm total pressure O_2/N_2 mixtures.

oxidation to provide an upper bound on the particle temperature. The particle temperature elevation is seen to increase with increasing ambient temperature and with increasing oxygen concentration. Negligible particle temperature elevation is seen below about 2200 K. The particle is assumed to be initially in equilibrium with the bath gas.

Figures 10 and 11 show similar results for 0.1 and 0.01 atm, respectively. Note the change in the temperature elevation scale, indicating that the particle temperature elevation increases with decreasing pressure. At the lowest pressure, substantial particle temperature elevation is computed down to 1600–1800 K ambient temperature.

The pressure dependence of the particle temperature elevation is shown directly in Fig. 12. This figure shows a 50-nm-diam particle combusting with pure O_2 at 1.0, 0.1, and 0.01 atm. The particle is assumed to be initially in equilibrium with the 2200-K bath gas. At 1.0 atm, there is negligible particle temperature increase. At 0.1 atm the particle temperature reaches a plateau at about 250 K above the gas temperature, with a small increase at burnout. At 0.01 atm, the particle

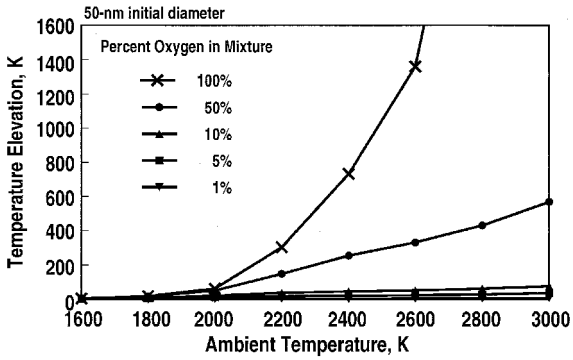

Fig. 10 Particle temperature elevation at burnout for 0.10-atm total pressure O_2/N_2 mixtures.

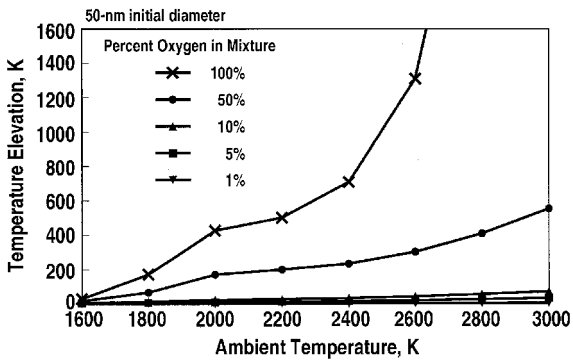

Fig. 11 Particle temperature elevation at burnout for 0.01-atm total pressure O_2/N_2 mixtures.

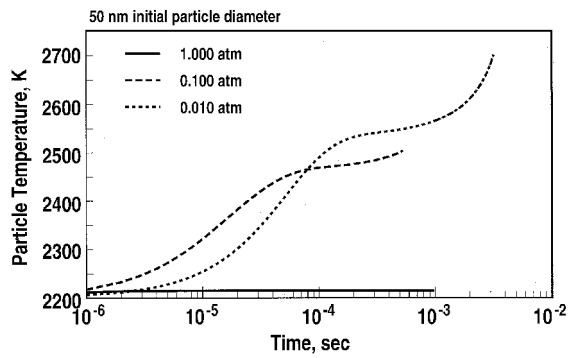

Fig. 12 Particle temperature history in 100% molecular oxygen for various pressures.

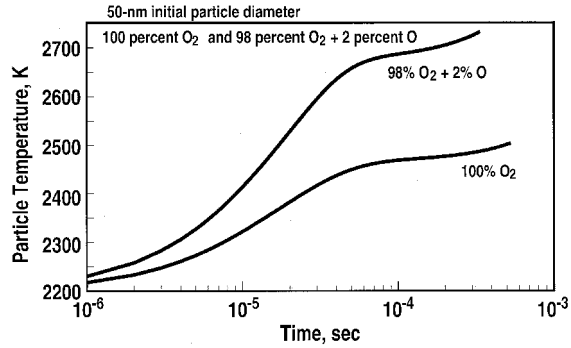

Fig. 13 Particle temperature history in O_2 and O_2/O mixture at 0.10 atm.

temperature reaches a plateau at about 300 K above the ambient gas temperature, with a rapid increase at burnout. It is interesting to note that the particle burns out faster at 0.1 atm than at 1.0 atm, even though the collision frequency is an order of magnitude greater at 1.0 atm. This seemingly counterintuitive behavior is explained by the particle temperature elevation at 0.1 atm. As the particle temperature rises, the collision efficiency increases (see Fig. 5), which produces still higher temperatures. This feed-forward process causes the collision efficiency-collision frequency product to be greater at 0.1 atm than at 1.0 atm. Therefore, the particle lifetime is shorter at 0.1 atm.

Figure 13 shows the particle temperature history of a 50-nm-diam particle oxidizing at 0.1 atm in two ambient gas compositions: 100% O_2 and 98% O_2/2% O. The Cadman et al.[22] rates are used for O_2 and the Rosner and Allendorf[24] rates are used for O. The particle is assumed to be initially in equilibrium with the 2200 K bath gas. The addition of this small amount of atomic oxygen causes an increase of 200 K in the particle temperature. Collisions with O are efficient and very exothermic.

Conclusions and Recommendations

Soot particles will experience significant rarefaction effects while oxidizing at moderate pressure conditions. The conclusion that small oxidizing soot particles will remain in thermal equilibrium with the surrounding gas is invalid. This assumption follows from the assumption of continuum flow, which predicts that the convective heat transfer coefficient is independent of pressure, inversely proportional to particle size, and dependent on the gas thermal conductivity. For sufficiently small particle size, the particle *Kn* is large and the particles experience free molecular flow. For free molecular flow the convective heat transfer coefficient is dependent on pressure and independent of particle size and gas thermal conductivity. Under these conditions, energy addition by oxidation can overcome the convective loss and drive the soot particle temperature above the ambient gas temperature.

Small particle thermal nonequilibrium is favored by low-pressure, high-ambient temperature, and high relative concentration of the oxidizing species. Collisions with inert species such as N_2 are very effective at reducing the particle temperature. Small amounts of atomic oxygen can cause large increases in particle temperature.

The collision efficiency and products of reaction of other important oxidizing species need to be determined. For example, the current flame literature indicates that OH is a principal soot oxidizer in flames. Reaction rates of OH with soot have been derived, but no unambiguous measurements of the products have been made. Without knowledge of the products, no statement about the exothermicity or endothermicity of the reaction can be made.

Oxidation is not the only mechanism for energy release on the surface of soot particles. Soot particles present a potential catalytic surface for the exothermic recombination of flame

radicals. The free molecular energy equation removes the dominance of the convective loss and means that the determination of soot particle temperature may be subject to more effects than previously recognized.

Soot oxidation and catalytic recombination should be studied in low pressure flames to confirm and quantify the rarefaction effects. Shock-tube studies of soot oxidation rates should include emission measurements to infer particle temperature as well as absorption measurements to infer particle consumption rates.

Finally, it is important to note that this theory is fully free molecular. No gas–gas collisions are considered. Direct simulation Monte Carlo calculations should be done to assess the importance of gas–gas collisions for a variety of particle Knudsen numbers and temperatures.

Acknowledgments

The research reported herein was performed by the Arnold Engineering Development Center (AEDC), Air Force Materiel Command. Work and analysis for this research were performed by personnel of Sverdrup Technology, Inc., AEDC Group, Technical Services Contractor for AEDC.

References

[1]Glassman, I., *Combustion*, 2nd ed., Academic, Orlando, FL, 1987, pp. 386–410.

[2]Lixing, Z., *Theory and Numerical Modeling of Turbulent Gas-Particle Flows and Combustion*, CRC Press, Boca Raton, FL, 1993, pp. 73–85.

[3]Kanury, A. M., *Introduction to Combustion Phenomena*, Gordon and Breach, New York, 1975, pp. 200–216.

[4]Coffin, K. P., "Burning Times of Magnesium Ribbons in Various Temperatures," NACA TN-3332, Dec. 1954.

[5]Coffin, K. P., and Brokaw, R. S., "A General System for Calculating Burning Rates of Particles and Drops and Comparison of Calculated Rates for Carbon, Boron, Magnesium, and Isooctane," NACA TN-3929, Feb. 1957.

[6]Libby, P. A., and Blake, T. R., "Theoretical Study of Burning Carbon Particles," *Combustion and Flame*, Vol. 36, No. 2, 1979, pp. 139–169.

[7]Park, C., and Appleton, J. P., "Shock-Tube Measurements of Soot Oxidation Rates," *Combustion and Flame*, Vol. 20, No. 3, 1973, pp. 369–379.

[8]Brandt, O., and Roth, P., "Measurements of the High Temperature Oxidation Rate of Soot Particles," *Journal of Aerosol Science*, Vol. 19, No. 7, 1988, pp. 863–866.

[9]Roth, P., Brandt, O., and Von Gersum, S., "High Temperature Oxidation of Suspended Soot Particles Verified by CO and CO_2 Measurements," *23rd Symposium (International) on Combustion*, The Combustion Inst., Pittsburgh, PA, 1990, pp. 1485–1491.

[10]Von Gersum, S., and Roth, P., "Soot Oxidation in High Temperature N_2O/Ar and NO/Ar Mixtures," *24th Symposium (International) on Combustion*, The Combustion Inst., Pittsburgh, PA, 1992, pp. 999–1006.

[11]Kreith, F., *Principles of Heat Transfer*, 3rd ed., Harper and Row, New York, 1973, pp. 398–401.

[12]Incropera, F. R., and De Witt, D. P., *Fundamentals of Heat Transfer*, Wiley, New York, 1981, pp. 440–450.

[13]Kennard, E. H., *Kinetic Theory of Gases*, McGraw–Hill, New York, 1938, pp. 176–180.

[14]Oppenheim, A. K., "Generalized Theory of Convective Heat Transfer in a Free-Molecule Flow," *Journal of the Aeronautical Sciences*, Vol. 20, No. 1, 1953, pp. 49–58.

[15]Schaaf, S. A., and Chambré, P. L., *Flow of Rarefied Gases*, Princeton Univ. Press, Princeton, NJ, 1961, pp. 11–16.

[16]Simmons, F. S., and Spadaro, F. G., "Thermal Lag of Solid Carbon in Rocket Nozzle Flow," Western States Combustion Inst. Meeting, Paper 60-2, 25 April 1960.

[17]Gordon, S., and McBride, B. J., "Computer Program for the Calculation of Complex Chemical Equilibrium Compositions, Rocket Performance, Incident and Reflected Shocks, and Chapman-Jouget Detonations," NASA SP-273 and Supplements, March 1976.

[18]Present, R. D., *Kinetic Theory of Gases*, McGraw–Hill, New York, 1958, p. 222.

[19]Vincenti, W. G., and Kruger, C. H., *Introduction to Physical Gas Dynamics*, Krieger, Malabar, FL, 1965, pp. 15–23.

[20]Chase, M. W., Jr., Davies, C. A., Downey, J. R., Jr., Frurip, D. J., McDonald, R. A., and Syverud, A. N., *JANAF Thermochemical Tables*, 3rd ed., Vols. 1 and 2; also *Journal of Physical and Chemical Reference Data*, Vol. 14, 1985, Supplement 1, American Inst. of Physics, New York, 1986.

[21]Lee, S. C., and Tien, C. L., "Optical Constants of Soot in Hydrocarbon Flames," *18th Symposium (International) on Combustion*, The Combustion Inst., Pittsburgh, PA, 1981, pp. 1159–1166.

[22]Cadman, P., Cornish, R., and Denning, R. J., "The Oxidation of Soot Particulates in Shock Waves," *Current Topics in Shock Waves—17th International Symposium on Shock Waves and Shock Tubes, AIP Conference Proceedings 208*, American Inst. of Physics, New York, 1990, pp. 751–755.

[23]Nagle, J., and Strickland-Constable, R. F., "Oxidation of Carbon Between 1000–2000°C," *Proceedings of the 5th Conference on Carbon*, Pergamon, New York, 1961, pp. 154–164.

[24]Rosner, D. E., and Allendorf, H. D., "Comparative Studies of the Attack of Pyrolytic and Isotropic Graphite by Atomic and Molecular Oxygen at High Temperatures," *AIAA Journal*, Vol. 6, No. 4, 1968, pp. 650–654.

[25]Olander, D. R., Siekhaus, W., Jones, R., and Schwarz, J. A., "Reactions of Modulated Molecular Beams with Pyrolytic Graphite. I. Oxidation of the Basal Plane," *Journal of Chemical Physics*, Vol. 57, No. 1, 1972, pp. 408–420.

[26]Olander, D. R., Siekhaus, W., Jones, R., and Schwarz, J. A., "Reactions of Modulated Molecular Beams with Pyrolytic Graphite. II. Oxidation of the Prism Plane," *Journal of Chemical Physics*, Vol. 57, No. 1, 1972, pp. 421–433.

[27]Rosner, D. E., and Allendorf, H. D., "Kinetics of the Attack of Refractory Materials by Dissociated Gases," *Heterogeneous Kinetics at Elevated Temperatures, Proceedings of the International Conference in Metallurgy and Materials Science*, edited by G. R. Belton and W. L. Worrell, Plenum, New York, 1969.